

# Full-dimensionality quantum calculations of acetylene–vinylidene isomerization

Shengli Zou,<sup>a)</sup> Joel M. Bowman,<sup>b)</sup> and Alex Brown

Department of Chemistry and Cherry L. Emerson Center for Scientific Computation, Emory University, Atlanta, Georgia 30322

(Received 27 January 2003; accepted 10 March 2003)

The isomerization of acetylene to vinylidene is examined theoretically in full dimensionality (six degrees of freedom), using a new *ab initio* potential energy surface [S. Zou and J. M. Bowman, Chem. Phys. Lett. **368**, 421 (2003)]. Eigenfunctions and eigenvalues of the exact Hamiltonian, for zero total angular momentum, are obtained using a series of novel truncation/recoupling procedures that permits calculations up to very high energies. The Hamiltonian is given in diatom–diatom Jacobi coordinates, with the choice  $H_2-C_2$  for the two diatoms in order to exploit the full permutational symmetry of the problem. By examining expectation values of the eigenfunctions, a number of states are definitely identified with vinylidenelike characteristics. Corresponding calculations are also done for  $C_2D_2$ . Full dimensional simulations of the photodetachment spectra of  $C_2H_2^-$  and  $C_2D_2^-$  are done (within the Franck–Condon approximation) and compared to the experimental ones. For this calculation the ground vibrational state wave function of the anion is obtained using a new force field, based on high quality *ab initio* calculations, which are also briefly reported. © 2003 American Institute of Physics. [DOI: 10.1063/1.1571520]

## I. INTRODUCTION

Interest in acetylene–vinylidene isomerization, as a prototype of 1,2-H atom migration, is long-standing. The first experimental evidence for the existence of vinylidene was found in the pioneering photodetachment experiments of the vinylidene anion by the Lineberger group in the 1980s.<sup>1</sup> In that study, broad spectral features in the (low-resolution) photodetachment spectrum of the vinylidene anion were attributed to the formation of metastable vinylidene. The argument was made in that paper that vinylidene probably exists as a nonstationary state that would dephase and lose its identity on the order of picoseconds, due to the overlap of that state with the dense set of presumed delocalized acetylenic molecular eigenstates. However, the possibility of eigenstates with vinylidene characteristics could not definitely be ruled out, and an intensive search for such states was carried in the 1990s by Field and co-workers.<sup>2</sup> That group probed high energy states of acetylene using stimulated emission pumping spectroscopy. The spectra, which are above the barrier to form vinylidene, and which may contain signatures of a vinylidene species, are highly congested and very challenging to assign. Thus, no definitive assignments of vinylidene states could be made, and the issue was still clouded until 1998. In that year, Coulomb explosion experiments on the vinylidene anion were reported.<sup>3</sup> These experiments, although somewhat qualitative, indicated that the lifetime of a vinylidene state was of the order of microseconds or longer, much longer than the estimate given by the Lineberger group.

These experiments stimulated much theoretical work over roughly a twenty-year time frame. The first combined *ab initio* and dynamics study of vinylidene was reported by Carrington *et al.*<sup>4</sup> They determined a reaction path connecting the vinylidene minimum, isomerization barrier, and acetylene minimum and determined a vinylidene lifetime, semiclassically, of the order of picoseconds. This estimate was in accord with the experimental estimate of the Lineberger group. Subsequently, theoretical efforts focused on high quality *ab initio* calculations of the energetics and harmonic frequencies of the isomerization barrier and vinylidene minimum. The most accurate calculation of the isomerization saddle point and vinylidene structure was done recently at the CCSDT level of theory, with an extrapolation to the complete basis set limit.<sup>5</sup> The electronic barrier to isomerization was given in this work as 2.85 kcal/mol. A second-order perturbation theory anharmonic analysis of the vinylidene and vinylidene anion vibrational fundamentals was also reported, based on CCSD(T) calculations.<sup>6</sup> Significant corrections to harmonic frequencies were found, and these resulted in improved agreement with the peak positions in the photodetachment spectrum. Limited *ab initio* calculations have been reported in connection with recent dynamics calculations; these are reviewed in detail below. Until very recently there existed essentially one semiglobal potential spanning the acetylene and vinylidene minima and isomerization barrier, due to Carter *et al.*,<sup>7</sup> as modified slightly by Halonen *et al.*<sup>8</sup> The Carter–Halonen potential energy surface (PES) was based on earlier *ab initio* calculations and is considerably more accurate for the acetylene region than for vinylidene. Very recently, this PES has been modified again in the vinylidene region by Stanton to incorporate his new *ab initio* calculations.<sup>9</sup> A new, more accurate semiglobal poten-

<sup>a)</sup>Present address: Department of Chemistry, Northwestern University, 2145 Sheridan Road, Evanston, IL 60208-3133.

<sup>b)</sup>Electronic mail: bowman@euch4e.chem.emory.edu

tial has just been reported by two of us.<sup>10</sup> This potential is used in the present work and is briefly described in Sec. III.

The first multidimensional quantum dynamics study of vinylidene isomerization was reported by Germann and Miller,<sup>11</sup> who considered two and three degree-of-freedom models in vinylidene normal coordinates using the Carter–Halonen potential. Their goal was to obtain the microcanonical isomerization “resonances” for vinylidene in various initial vibrational states. The calculations employed a negative imaginary (“absorbing”) potential just beyond the isomerization barrier and in the acetylene region to avoid dealing with the large density of high-excited acetylene states. The use of this potential introduces a negative imaginary part to the energy eigenvalues, which can be interpreted as lifetimes (or equivalently resonance widths). However, in the case of a truly bound system such as vinylidene–acetylene, the eigenvalues are necessarily real, and thus this approach is not rigorously correct. Nevertheless, as shown by them it is very useful in assessing the relative metastability of modes of vibration of vinylidene.

Similar absorbing boundary conditions were used recently by Schork and Köppel<sup>12</sup> in extensive reduced dimensionality (up to five degrees-of-freedom) wavepacket simulations of the vinylidene anion photodetachment spectrum. These authors used “satellite” coordinates that were originally suggested by Wyatt and co-workers<sup>13</sup> in their quantum calculations of low-lying vibrational states of planar acetylene. A new *ab initio* potential [at the CCSD(T) level of theory] was also calculated; however, it was limited to the vinylidene and barrier region of the neutral and the anion. As in the Germann–Miller work, Shork and Köppel obtained lifetimes for a variety of vinylidene vibrational states. The results were quite dependent on the number of degrees of freedom considered. For example, for the zero-point level the lifetime in four and five degrees-of-freedom was reported as 46 and 293 picoseconds. The lifetimes for excited vibrational states ranged from sub-picoseconds to picoseconds. (By slightly adjusting the line widths in their calculations, they were able to obtain excellent agreement with the experimental photodetachment spectrum of the Lineberger group.) An important conclusion of this work was that the apparent lifetime of vinylidene in the zero-point level was longer than picoseconds. This supported, at least qualitatively, the conclusions of the more recent Coulomb explosion experiments mentioned above. These authors also noted long-time recurrences in the time-dependent correlation function and concluded that the isomerization is not a simple exponential decay, but involves significant barrier recrossing.

The same conclusion about significant barrier recrossing was reached in planar *ab initio* “direct-dynamics” (classical) calculations for fully deuterated vinylidene, reported by Carter and co-workers.<sup>14</sup> The potential energy was obtained “on-the-fly” at the CASSCF level of theory, and due to the heavy computational demands of this approach, only a small number of trajectories were done. These trajectories, which were initiated in the vinylidene configuration, exhibited significant recrossing of the isomerization barrier. (It should be noted that earlier classical trajectory calculations of highly excited planar acetylene were reported by Holme and Le-

vine, using a model potential energy surface.<sup>15</sup> These authors did not focus on the lifetime of vinylidene.)

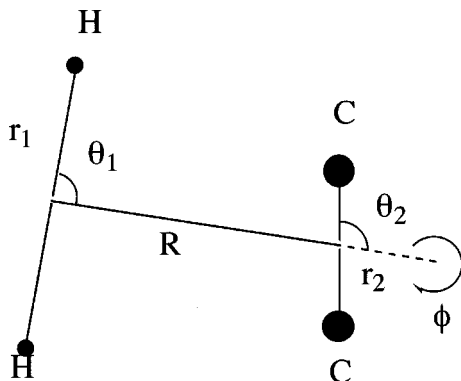
We recently reported four degree-of-freedom quantum calculations of high-energy molecular eigenstates of acetylene<sup>16</sup> using the Stanton–Carter potential. Eigenstates with clear vinylidene characteristics were found. A follow-up calculation in full dimensionality, using this potential, was reported as a Communication.<sup>17</sup> Again, eigenstates with very clear vinylidene characteristics were found. These two calculations were the first to present definitive theoretical evidence for the existence of vinylidene-like molecular eigenstates. This work stimulated Prosmi and Farantos to perform a nonlinear dynamics analysis of the periodic orbit structure of acetylene and vinylidene<sup>18(a)</sup> on the Stanton–Carter potential. They find strong evidence for stable periodic orbits in vinylidene, in support of the quantum calculations, and in agreement with their previous work<sup>18(b)</sup> on the original Carter potential.

In doing further work, specifically a calculation of the photodetachment spectrum, we discovered that the Stanton–Carter potential does not describe the vinylidene vibrations very well. In particular, the CC-stretch has an anomalously low harmonic frequency. As a result, we calculated a new *ab initio* potential energy surface for vinylidene–acetylene<sup>10</sup> as noted already. We have used this new potential in new full-dimensional calculations of highly excited C<sub>2</sub>H<sub>2</sub> as well as C<sub>2</sub>D<sub>2</sub> and present the results here. In addition, we calculated the photodetachment spectra of the corresponding anions (in the Franck–Condon approximation). To do that, a new *ab initio* force field for the vinylidene anion was calculated and from it the ground vibrational state anion wave function was obtained and used in the calculation of the photodetachment spectra.

The paper is organized as follows: The methods used and details of the calculations are given in Sec. II. The choice of coordinate system, Hamiltonian, and diagonalization–recoupling procedures are outlined in Secs. II A and II B. Section II C provides the details of the bases used for our calculations. Results and discussion are given in Sec. III, and we summarize and give our conclusions in Sec. IV.

## II. METHODS AND CALCULATION DETAILS

The exact quantum calculation of molecular eigenstates of C<sub>2</sub>H<sub>2</sub> (and C<sub>2</sub>D<sub>2</sub>) at energies above the threshold to access the vinylidene region of the potential to spectroscopic accuracy, i.e., a few wave numbers, is currently not feasible by any method. However, this level of accuracy is almost certainly not necessary in order to determine whether there *exist* molecular eigenstates with vinylidene characteristics. The methods we developed were done with this in mind, and thus they have some novel features. In general, we seek to develop the most compact representation of the Hamiltonian, by using reduced dimensionality bases that are obtained by a sequence of diagonalization/recoupling procedures. These are described fully below, but first we discuss the choice of coordinate system and give the corresponding exact Hamiltonian.

FIG. 1. Diatom-diatom Jacobi coordinates of  $C_2H_2$ .

### A. Coordinate system

The choice of coordinates is clearly very important in the study of isomerization. As noted in the previous section “satellite” coordinates<sup>13</sup> were used by Shork and Köppel.<sup>12</sup> These consist of a CC position vector and two vectors for the H atoms relative to the geometric center of the CC bond. As shown by Bentley *et al.*,<sup>13</sup> the full symmetry of the potential can be exploited in these coordinates; however, not in a straightforward analytical fashion. Instead of using these coordinates, we chose  $C_2-H_2$  diatom-diatom Jacobi coordinates, which are shown in Fig. 1. There is a threefold advantage to using these coordinates. First, the exact Hamiltonian is known and it is relatively simple, second it is easy to exploit the full permutational symmetry of the molecule, and third the isomerization from acetylene to vinylidene is described by a “simple” process in which  $R$  increases from zero,  $r_1$  decreases (significantly), and  $\theta_2$  changes from  $\pi/2$  to 0 (or  $\pi$ ). Thus, there are two equivalent vinylidene minima, as we have noted previously.<sup>17</sup> Note also that acetylene and vinylidene have planar minima, corresponding to a dihedral angle,  $\phi$ , equal to zero and the CC distance,  $r_2$ , changes very little for these minima.

While  $C_2-H_2$  diatom-diatom Jacobi coordinates are clearly much better suited to describe vinylidene than low-energy acetylene states, we have demonstrated previously that they can yield accurate vibrational energies for acetylene states.<sup>10,17</sup> A better set of diatom-diatom Jacobi coordinates to describe acetylene is the CH-CH coordinates. These have been used by Guo and co-workers<sup>19</sup> in full dimensional calculations of acetylene states and earlier by Liu and Muckerman in planar calculations of acetylene states.<sup>20</sup>

### B. The truncation-recoupling procedure

The full dimensional, body-fixed Hamiltonian for diatom-diatom Jacobi coordinates is<sup>21,22</sup>

$$\hat{H} = \frac{(\hat{J} - \hat{j}_{12})^2}{2\mu_R R^2} + \frac{\hat{j}_1^2}{2\mu_1 r_1^2} + \frac{\hat{j}_2^2}{2\mu_2 r_2^2} - \frac{\hbar^2}{2\mu_R} \frac{\partial^2}{\partial R^2} - \frac{\hbar^2}{2\mu_{r_1}} \frac{\partial^2}{\partial r_1^2} - \frac{\hbar^2}{2\mu_{r_2}} \frac{\partial^2}{\partial r_2^2} + V(\mathbf{r}_1, \mathbf{r}_2, \mathbf{R}), \quad (1)$$

where  $\mu_1$ ,  $\mu_2$ , and  $\mu_R$  are the usual reduced masses corresponding to the distances  $r_1$ ,  $r_2$ , and  $R$ , respectively,  $\hat{J}$  is the total angular momentum operator,  $\hat{j}_1$  and  $\hat{j}_2$  are the rotational angular momentum operators associated with the angular variables of the vectors  $\mathbf{r}_1$  and  $\mathbf{r}_2$ , and  $\hat{j}_{12}$  is  $\hat{j}_1 + \hat{j}_2$ . As usual, the body-fixed  $z$ -axis is along the vector  $\mathbf{R}$ . In this frame, the angles  $\theta_1$  and  $\theta_2$  are the polar angles of the vectors  $\mathbf{r}_1$  and  $\mathbf{r}_2$ , respectively, and  $\phi$  is the dihedral angle  $\phi_1 - \phi_2$ , where  $\phi_1$  and  $\phi_2$  are the azimuthal angles of  $\mathbf{r}_1$  and  $\mathbf{r}_2$  in the body-fixed frame.

To simplify the problem, we consider only zero total angular momentum, and thus

$$\hat{H}^{J=0} = \frac{\hat{j}_{12}^2}{2\mu_R R^2} + \frac{\hat{j}_1^2}{2\mu_1 r_1^2} + \frac{\hat{j}_2^2}{2\mu_2 r_2^2} - \frac{\hbar^2}{2\mu_R} \frac{\partial^2}{\partial R^2} - \frac{\hbar^2}{2\mu_{r_1}} \frac{\partial^2}{\partial r_1^2} - \frac{\hbar^2}{2\mu_{r_2}} \frac{\partial^2}{\partial r_2^2} + V(\mathbf{r}_1, \mathbf{r}_2, \mathbf{R}). \quad (2)$$

(For simplicity we drop the  $J=0$  superscript, hereafter.) The approach we take to obtain eigenfunctions and eigenvalues of this Hamiltonian is based on a reduced dimensionality, truncation-recoupling approach that we and others have developed over the years.<sup>23-25</sup> The objective is to keep the final Hamiltonian matrix as small as possible, and the basic strategy is to use bases that are eigenfunctions of reduced dimensionality Hamiltonians. Typically, these Hamiltonians are obtained from the full dimensional Hamiltonian by fixing some coordinates at reference values corresponding to the minimum on the potential energy surface. Thus, these bases are termed numerical, or potential optimized. In the simplest version, these bases are functions of a single coordinate, i.e., one-dimensional (1D) basis functions. A more effective approach is to use multidimensional numerical bases, which can result in a significantly more compact final Hamiltonian matrix.

Most applications of numerical bases have been to problems where one is interested in obtaining eigenfunctions in the vicinity of a potential minimum. However, this approach cannot be used to study acetylene-vinylidene isomerization, which involves large amplitude motion in all degrees of freedom, except the CC-stretch. Below, we describe a modification of the numerical basis truncation-recoupling approach that does permit a description of this isomerization. The key feature of this novel approach is the use of a reduced dimensionality potential that is minimized with respect to other degrees of freedom, such that the resulting potential contains both the acetylene and vinylidene minima.

In the first step, we determine a reduced dimensionality basis in the three angular coordinates  $\theta_1$ ,  $\theta_2$ , and  $\phi$ , defined above, and depicted in Fig. 1. The general approach we have programmed, and used previously,<sup>17</sup> is to determine this basis as eigenfunctions of the following three-dimensional (3D) Hamiltonian

$$\hat{H}_{3D} = \frac{\hat{j}_{12}^2}{2\mu_R R_{\text{cut}}^2} + \frac{\hat{j}_1^2}{2\mu_1 r_{1e}^2} + \frac{\hat{j}_2^2}{2\mu_2 r_{2e}^2} + V_{3D}(\theta_1, \theta_2, \phi), \quad (3)$$

where  $V_{3D}$  is the potential for  $\theta_1$ ,  $\theta_2$ , and  $\phi$ , with  $R$  fixed at  $R_{\text{cut}}$ , and minimized with respect to the remaining variables  $r_1$  and  $r_2$ . In the calculations reported previously,<sup>17</sup> we fixed  $R_{\text{cut}}$  near the value at the isomerization barrier. With this choice of  $R_{\text{cut}}$ ,  $V_{3D}$  “contains” the acetylene and vinylidene regions of the full potential. However, this particular choice of  $R_{\text{cut}}$  gives a much better description of the vinylidene minimum than it does of the acetylene one. (In calculations of low-lying states of acetylene, we chose the value 0.5 bohr,<sup>10</sup> which is close to the expectation values of  $R$  in the ground acetylene state.)

In the present calculations we do not use a potential in  $\hat{H}_{3D}$ , i.e.,  $V_{3D}=0$ , and thus the eigenfunctions are the well-known, body-fixed angular functions  $y_{j_1 j_2}^{j_{12} K}(\theta_1, \theta_2, \phi)$ ,<sup>22</sup> which are eigenfunctions of  $J_{12}^2$ ,  $J_1^2$ , and  $J_2^2$ , and where  $K$  is the projection quantum number of the total angular momentum on the body-fixed  $z$ -axis. (The eigenvalues are the analogs of rigid-rotor ones, with radial lengths chosen as follows:  $R_{\text{cut}}=2.0$  bohr, while  $r_1=r_{1e}$  and  $r_2=r_{2e}$ , i.e., the equilibrium values for vinylidene.) The explicit construction of these functions is given by the standard expression

$$y_{j_1 j_2}^{j_{12}, K}(\theta_1, \theta_2, \phi) = \sum_{m_1} C(j_1 j_2 j_{12}; m_1 (K - m_1) K) \times \Theta_{j_1, m_1}(\theta_1) \Theta_{j_2, K - m_1}(\theta_2) \frac{e^{im_1 \phi}}{\sqrt{2\pi}}, \quad (4)$$

where  $\Theta_{j_1, m_1}(\theta_1)$ , and  $\Theta_{j_2, K - m_1}(\theta_2)$  are normalized associated Legendre polynomials, and  $C(j_1 j_2 j_{12}; m_1 (K - m_1) K)$  are the Clebsch–Gordan coefficients.

To determine the parity and symmetry properties of these body-fixed angular functions it is necessary to relate them to space-fixed ones by the general expression

$$Y_{j_1 j_2 j_{12} K}^{JM}(\Phi, \Theta, \theta_1, \phi_1, \theta_2, \phi_2) = \tilde{D}_{MK}^{J*}(\Phi, \Theta, \phi_2) y_{j_1 j_2}^{j_{12} K}(\theta_1, \theta_2, \phi), \quad (5)$$

where  $\tilde{D}_{MK}^{J*}(\Phi, \Theta, \phi_2)$  is the normalized Wigner rotation matrix which rotates the body-fixed wave function to the space-fixed wave function and  $\Phi$  and  $\Theta$  are spherical polar angles of  $\mathbf{R}$  in the space-fixed frame.  $\phi_1$  and  $\theta_1$  and  $\phi_2$  and  $\theta_2$  are the spherical polar angles of  $\mathbf{r}_1$  and  $\mathbf{r}_2$  in the body-fixed frame, whose  $z$ -axis coincides with the vector  $\mathbf{R}$ , cf. Fig. 1, and  $\phi = \phi_1 - \phi_2$  is the dihedral angle. As is well-known,<sup>21,22</sup> the parity-adapted angular functions for arbitrary  $J$  and  $K$  are given by

$$Y_{j_1 j_2 j_{12} K}^{JM \varepsilon}(\Phi, \Theta, \theta_1, \phi_1, \theta_2, \phi_2) = \frac{1}{\sqrt{2(1 + \delta_{K0})}} (Y_{j_1 j_2 j_{12} K}^{JM}(\Phi, \Theta, \theta_1, \phi_1, \theta_2, \phi_2) + \varepsilon (-1)^{j_1 + j_2 + j_{12} + J} Y_{j_1 j_2 j_{12} - K}^{JM}(\Phi, \Theta, \theta_1, \phi_1, \theta_2, \phi_2)), \quad (6)$$

where  $\varepsilon$  represents the parity of the wave function, i.e.,

TABLE I. Correspondence between the  $j_i$ -dependent parity blocks and the irreducible representations for  $G_8$  (acetylene and vinylidene) and  $C_{2V}$  (vinylidene).

$j_1 + j_2 + j_{12}$	$j_1$	$j_2$	$j_{12}$	$G_8$	$C_{2V}$
even	even	even	even	$A'_1$	$A_1$
	even	odd	odd	$B'_2$	$A_1$
	odd	even	odd	$B''_2$	$B_2$
odd	odd	odd	even	$A'_1$	$B_2$
	even	even	odd	$A'_2$	$A_2$
	even	odd	even	$B'_1$	$A_2$
	odd	even	even	$B''_1$	$B_1$
	odd	odd	odd	$A''_2$	$B_1$

$$\hat{P} Y_{j_1 j_2 j_{12} K}^{JM \varepsilon}(\Phi, \Theta, \theta_1, \phi_1, \theta_2, \phi_2) = \varepsilon Y_{j_1 j_2 j_{12} K}^{JM \varepsilon}(\Phi, \Theta, \theta_1, \phi_1, \theta_2, \phi_2), \quad (7)$$

where  $\hat{P}$  is the parity operator and  $\varepsilon = \pm 1$ .

In the present case where  $J=0$ ,  $K$  and  $M$  must be zero,  $\tilde{D}_{00}^{0*}(\Phi, \Theta, \phi_2)$  equals one and thus the parity-adapted functions, denoted,  $y_{j_1 j_2}^{j_{12} \varepsilon}(\theta_1, \theta_2, \phi)$ , are given by

$$y_{j_1 j_2}^{j_{12} \varepsilon}(\theta_1, \theta_2, \phi) = (1 + \varepsilon (-1)^{j_1 + j_2 + j_{12}}) y_{j_1 j_2}^{j_{12} K=0}(\theta_1, \theta_2, \phi). \quad (8)$$

Thus, for even parity states, i.e.,  $\varepsilon=1$ ,  $j_1 + j_2 + j_{12}$  must be even, and for odd parity states,  $j_1 + j_2 + j_{12}$  must be odd. Using the parity of the wave functions, the Hamiltonian matrix can be separated into two different parity blocks depending on whether  $j_1 + j_2 + j_{12}$  is even or odd. This symmetry and block structure of the Hamiltonian matrix is general for all tetra-atomic molecules. Additional symmetries exist for  $C_2H_2$  due to permutational invariance of the Hamiltonian with respect to interchange of the two H atoms or the two C atoms. The relevant complete nuclear permutation inversion (CNPI) group is  $G_8$  and thus the Hamiltonian matrix can be separated into eight different blocks belonging to irreducible representations  $A'_1$ ,  $A''_1$ ,  $A'_2$ ,  $A''_2$ ,  $B'_1$ ,  $B''_1$ ,  $B'_2$ , and  $B''_2$ . It is fairly straightforward to show that these irreps correspond to particular restrictions on  $j_1$ ,  $j_2$ , and  $j_{12}$  and these are indicated in Table I.

Making full use of the CNPI symmetry, the Hamiltonian matrix is eightfold block diagonal, which greatly facilitates a direct-diagonalization approach to obtain eigenvalues and eigenfunctions. In addition, the evaluation of potential matrix elements over the angular degrees of freedom can be simplified using this symmetry. The integration range is, as usual,  $-1$  to  $1$  for  $\cos \theta_1$  and  $\cos \theta_2$  and  $0$  to  $\pi$  for  $\phi$  (using a parity-adapted basis). Using the permutational symmetry of the two diatoms, the integration range can be halved for the angles  $\theta_1$  and  $\theta_2$  resulting in an additional savings of a factor of 4 in doing the numerical integration.

In the next step, we obtain eigenfunctions of the following four-dimensional (4D) Hamiltonian

TABLE II. Geometry (bohrs and degrees) and energies ( $\text{cm}^{-1}$ ) of stationary points on the new *ab initio* potential.<sup>a</sup>  $R_{\text{CH}_1}$  and  $R_{\text{CH}_2}$  are the two CH bond lengths and  $\theta_{\text{H}_1\text{-C-C}}$  and  $\theta_{\text{H}_2\text{-C-C}}$  are the two HCC bond angles.

	Vinylidene	Acetylene	Saddle Pt
$R_{\text{CH}_1}$	2.054	2.011	2.028
$R_{\text{CH}_2}$	2.054	2.011	2.568
$R_{\text{CC}}$	2.470	2.287	2.385
$\theta_{\text{H}_1\text{-C-C}}$	120	180	175
$\theta_{\text{H}_2\text{-C-C}}$	120	180	55
$R$	2.264	0	
$r_{\text{HH}}=r_1$	3.555	6.308	
$r_{\text{CC}}=r_2$	2.469	2.287	
Energy	15410	0	16382

<sup>a</sup>Reference 10.

$$\hat{H}_{4\text{D}} = \hat{H}_{3\text{D}} + \hat{j}_{12}^2 \left( \frac{1}{2\mu_{\text{R}}R^2} - \frac{1}{2\mu_{\text{R}}R_{\text{cut}}^2} \right) - \frac{\hbar^2}{2\mu_{\text{R}}} \frac{\partial^2}{\partial R^2} + V_{4\text{D}}(\theta_1, \theta_2, \phi, R) - V_{3\text{D}}(\theta_1, \theta_2, \phi), \quad (9)$$

where  $V_{4\text{D}}(\theta_1, \theta_2, \phi, R)$  is the potential in the four coordinates  $R$ ,  $\theta_1$ ,  $\theta_2$ , and  $\phi$ , and minimized with respect to the remaining  $r_1$  and  $r_2$  variables. [In the present calculations  $V_{3\text{D}}(\theta_1, \theta_2, \phi)$  is zero and hereafter we eliminate reference to it.] Note that  $V_{4\text{D}}(\theta_1, \theta_2, \phi, R)$  contains both the acetylene and vinylidene minima, with the correct energetics, and thus the eigenfunctions of  $\hat{H}_{4\text{D}}$  must span large amplitude motions. The choice of the basis to represent these eigenfunctions must therefore be able to describe large amplitude motion in these variables. Clearly the eigenfunctions of  $\hat{H}_{3\text{D}}$  satisfy this requirement for the angular variables. For a basis in  $R$ , we chose simple sine functions spanning a range 0 to  $R_{\text{max}}$ . Thus, the final 4D basis is a direct-product of symmetry-adapted functions  $y_{j_1 j_2}^{j_{12}^e}(\theta_1, \theta_2, \phi)$  with sine functions in  $R$ . (This resulting in the largest Hamiltonian matrix in the calculation.)

Finally, eigenfunctions of  $\hat{H}_{4\text{D}}$  are combined with a 2D basis in  $r_1$  and  $r_2$  (the HH and CC stretches) to obtain the final 6D basis for the full dimensional Hamiltonian. In the spirit of using reduced dimensionality Hamiltonians, this 2D basis consists of eigenfunctions of a 2D Hamiltonian

$$\hat{H}_{2\text{D}} = -\frac{\hbar^2}{2\mu_{r_1}} \frac{\partial^2}{\partial r_1^2} - \frac{\hbar^2}{2\mu_{r_2}} \frac{\partial^2}{\partial r_2^2} + V_{2\text{D}}(r_1, r_2), \quad (10)$$

where  $V_{2\text{D}}(r_1, r_2)$  is a reference 2D potential. For the present calculations, where  $r_1$  ( $r_{\text{HH}}$ ) must span a large range in going from acetylene to vinylidene (cf. Table II below) we used a basis of sine functions. In  $r_2$  ( $r_{\text{CC}}$ ), we used a relatively small numerical basis obtained from a 1D Hamiltonian with a potential given by a cut in  $r_2$  with all other coordinates fixed at the vinylidene equilibrium.

The final, exact 6D Hamiltonian is

$$\hat{H}_{6\text{D}} = \hat{H}_{4\text{D}} + \hat{H}_{2\text{D}} + \hat{j}_1^2 \left( \frac{1}{2\mu_{r_1}r_1^2} - \frac{1}{2\mu_{r_1}r_{1e}^2} \right) + \hat{j}_2^2 \left( \frac{1}{2\mu_{r_2}r_2^2} - \frac{1}{2\mu_{r_2}r_{2e}^2} \right) + V_{6\text{D}}(\theta_1, \theta_2, \phi, R, r_1, r_2) - V_{4\text{D}}(\theta_1, \theta_2, \phi, R) - V_{2\text{D}}(r_1, r_2), \quad (11)$$

where  $V_{6\text{D}}(\theta_1, \theta_2, \phi, R, r_1, r_2)$  is the full 6D potential.

### C. Basis sets

The details of the bases used in the present calculations are as follows: For each symmetry block, the maximum value of  $j_1$  and  $j_2$  was 26 for even states and 27 for odd states and the integration over  $\theta_1$  and  $\theta_2$  was done with 36 Gauss–Legendre quadrature points. The maximum value of  $m_1$  in Eq. (4) was its maximum possible value, i.e., 26 or 27 and the number of quadrature points in the dihedral angle  $\phi$  was 59. The range of  $j_{12}$  is  $|j_1 - j_2|$  to  $j_1 + j_2$ , and where both  $j_1$  and  $j_2$  are even this resulted in 1834 3D angular functions. These were combined with 24 sine functions for  $R$  (at 30 quadrature points) in the range 0–5.0 bohr. The order of the resulting 4D Hamiltonian matrix is 44 016 which used 15G of memory and required 47 hours of CPU time to obtain 300 eigenvalues and eigenfunctions on an HP ES45 workstation. For  $\text{C}_2\text{H}_2$ , convergence tests indicate that 4D eigenvalues for vinylidenelike states are converged to within about  $1 \text{ cm}^{-1}$  using this basis. The 2D basis in  $r_{\text{HH}}$  and  $r_{\text{CC}}$  was a direct product of 24 sine functions at 30 quadrature points for  $r_{\text{HH}}$  in the range 2.1–8.5 bohr and 6 numerical functions at 12 quadrature points for  $r_{\text{CC}}$  in the range 1.8–3.5 bohr.

Once the 4D and 2D bases were obtained, they were combined to obtain the full 6D basis used in the final determination of the eigenvalues and eigenfunctions. The goal is to obtain eigenvalues and, very importantly, eigenfunctions of the 6D Hamiltonian at energies above the threshold for formation of vinylidene. Even with the reduced dimensionality strategy described in Sec. II B, it was still a very demanding task to obtain all eigenstates to within “spectroscopic” accuracy at these high energies. For example, for  $\text{C}_2\text{H}_2$  a direct-product of the two bases, 144 2D functions and roughly 300 4D functions would result in a final matrix that is still too large for us to consider. Further, for  $\text{C}_2\text{D}_2$  many more 4D functions would be needed to reach the vinylidene threshold. In light of this, we have chosen to focus on obtaining vinylidene states to good accuracy, at the expense of this level of accuracy for highly excited acetylenic states. To do this we adopted a strategy of only using that part of the 4D basis with energies that span the energy range of vinylidene states. For all calculations, the entire 2D basis (144 functions) was utilized. In our preliminary report,<sup>17</sup> we used 80 4D states, the first of which is 10 states below the energy of the lowest-lying vinylidenelike 4D state, i.e., states 155–235. This resulted in moderately sized (of order 10 000) final 6D Hamiltonian matrices. Subsequently, we ported our code to an ES45 HP/alpha with 32G of RAM and have been able to extend the size of matrices to the order of 40 000.

This has enabled us to use a much larger 4D basis here. Specifically, most of the results we present in the next section were obtained using 150 4D basis functions spanning 20 states below the lowest energy 4D vinylidene state to 130 states above it, i.e., 4D states 145–295.

In order to test this approach we also did calculations with a complete 4D basis that begins with the lowest energy state of acetylene and terminates with an energy state well above the isomerization threshold, i.e., states 1–235. Using this large basis we could test the accuracy of a truncated basis of 80 4D states, i.e., states 155–235. (This is the size of the 4D basis used previously.<sup>17</sup>) We obtained a zero-point vinylidene wave function with an energy only  $0.6\text{ cm}^{-1}$  higher than the one obtained using the “full” (1–235) 4D basis (the identification of the vinylidene states is discussed in detail in Sec. III). Also, the energy differences for the fundamentals of  $A'_1$  symmetry ( $\nu_1$ ,  $\nu_2$ , and  $\nu_3$ ) are all within  $1\text{ cm}^{-1}$ . These comparisons indicate that the approach of using a subset of high energy 4D states is reasonable for obtaining vinylidene states; however, it clearly is not an accurate method for acetylene states. (We present additional results using these two bases in the next section.)

Having validated the approach of using a subset of the 4D basis for vinylidene states, we decided to use the partial basis of 150 4D states instead of the complete basis of 235 4D states because additional 4D vinylidenelike states could be used in the basis of 150 4D states. As expected, we found that the final 6D vinylidenelike states have somewhat lower energies than the results obtained with either the 80 4D basis or the 235 4D basis. Thus, we believe that the vinylidene energies reported below are close to being of “spectroscopic” accuracy, i.e., converged to within  $10\text{ cm}^{-1}$  or less. It must be noted that density of states obtained with the smaller 150 4D basis is smaller than then one using the complete basis of 235 4D states. This is discussed in more detail in the next section.

As extensive testing of the theoretical method has been performed for  $\text{C}_2\text{H}_2$ , less extensive testing was done for  $\text{C}_2\text{D}_2$ . The final  $\text{C}_2\text{D}_2$  results reported have been carried out with the same basis parameters as for  $\text{C}_2\text{H}_2$ , described in detail above. The one change is that we could not use all the 4D states, starting with the lowest energy one. (In order to perform a calculation using a 4D basis that begins with the lowest energy state and terminates with the maximum energy state used in the truncated 4D calculation, described below, would require 500 4D basis functions and the resulting 6D H-matrix would be of order 72 000.) Instead we adopted the strategy of using a subset of 4D states that span the vinylidene energy region as was done for  $\text{C}_2\text{H}_2$ . We used 230 4D states which span a smaller energy range,  $2985\text{ cm}^{-1}$ , starting with a state  $541\text{ cm}^{-1}$  below the first 4D vinylidene state, than in  $\text{C}_2\text{H}_2$ , where the 150 4D states span  $3315\text{ cm}^{-1}$  with the first state  $509\text{ cm}^{-1}$  below the first 4D vinylidene state. For the  $\text{C}_2\text{D}_2$  calculations, these 230 4D functions were combined with 144 2D functions resulting in a final H-matrix of order 33 120.

The results of these 6D calculations are given in the next section. In addition we used the 6D eigenfunctions to simulate the photodetachment spectra of  $\text{C}_2\text{H}_2^-$  and  $\text{C}_2\text{D}_2^-$  in the

Franck–Condon approximation. This simulation requires a wave function for the ground vibrational state of the anion(s). Rather than use an approximate harmonic model for this wave function, we calculated a new *ab initio* anion potential and numerically obtained the ground vibrational state wave function on the same 6D quadrature grid used in the 6D calculations of the neutral system. The details of these anion calculations are briefly given in the next section.

### III. RESULTS AND DISCUSSION

#### A. Potential energy surface

In our preliminary report of vinylidene states,<sup>17</sup> we used the Stanton–Carter potential, which is basically a modification of the Carter potential to improve the geometry and energetics of the isomerization barrier and vinylidene minimum. However, as noted in the Introduction, this potential does not give a good description of CC stretch of vinylidene. Thus, we decided to construct a new *ab initio* potential using a high level method and basis. This has been done and already reported.<sup>10</sup> Roughly 10 000 *ab initio* calculations were done and accurately fit by a least-squares method. Detailed properties of this new potential, and a calculation of low-lying acetylene vibrational states have already been reported,<sup>10</sup> and so only the most salient properties of this new potential are given in Table II. The coordinates used in the table include the usual bond lengths and bond angles and also the relevant Jacobi distances  $R$ ,  $r_1$ , and  $r_2$ . Note the large change in the values of  $R$  and  $r_1$  ( $r_{\text{HH}}$ ) for the acetylene and vinylidene minima. Thus, the expectation values of these two distances play signature roles in characterizing molecular eigenstates, which we examine next.

#### B. Energies and expectation values

As stated above, the goal of the present calculations is to investigate the nature of excited vibrational states with energies in excess of the threshold for formation of vinylidene. Thus, we do not compare energy eigenvalues to high-resolution experimental data that have determined vibrational energies of acetylene.<sup>2</sup> Instead we focus on properties of high-energy molecular eigenstates of  $\text{C}_2\text{H}_2$  and  $\text{C}_2\text{D}_2$ .

The calculations reported here are mainly for the  $A'_1$  symmetry block in  $G_8$ , i.e., the  $A_1$  symmetry block in  $C_{2v}$ , since these are the states that are observed in the photodetachment spectra. Unless specified otherwise the results presented for  $\text{C}_2\text{H}_2$  were obtained with the partial basis of 150 4D functions. For  $\text{C}_2\text{D}_2$ , all results were obtained using the partial basis of 230 4D functions.

To characterize the molecular eigenstates, we calculated, as before,<sup>16,17</sup> the expectation values of all six coordinates; however, here we focus on  $\langle R \rangle$  and  $\langle r_{\text{HH}} \rangle$  since these are the most different for acetylene and vinylidene, as already noted. For states with energies below the threshold for vinylidene formation (roughly  $20\,000\text{ cm}^{-1}$  above the acetylene minimum),  $\langle R \rangle$  gradually increases from around 0.5 to nearly 1.0 bohr and  $\langle r_{\text{HH}} \rangle$  fluctuates around 6.3 bohr, which is the equilibrium value at the acetylene minimum. (As a consequence

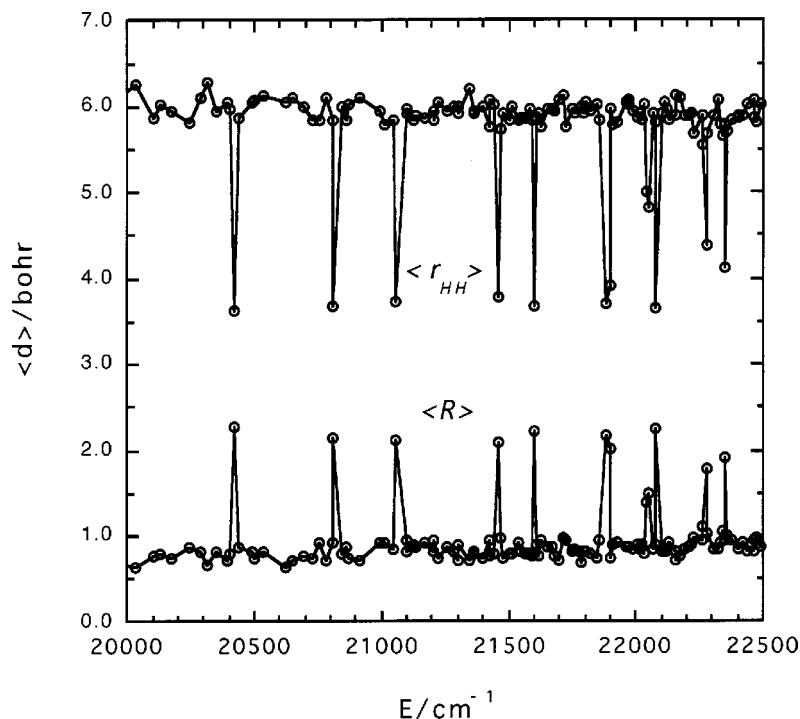


FIG. 2. Expectation values of the radial coordinates  $r_{HH}$  and  $R$  for six degree-of-freedom molecular eigenstates of  $C_2H_2$  (of  $A'_1$  symmetry) in the high-energy region.

of the uncertainty principle  $\langle R \rangle$  cannot equal zero, the equilibrium value, since the physical range of  $R$  must be greater than or equal to zero.)

### 1. $C_2H_2$

The expectation values  $\langle R \rangle$  and  $\langle r_{HH} \rangle$  for  $C_2H_2$  in the energy range of interest are plotted in Fig. 2 as a function of the energy above the acetylene minimum. As seen, there are a number of states with  $\langle R \rangle$  and  $\langle r_{HH} \rangle$  very different from values that are characteristic of acetylene. For these states  $\langle R \rangle$  is roughly equal to 2.4 bohr and  $\langle r_{HH} \rangle$  is roughly equal to 3.5 bohr. These values are quite close to the equilibrium values of  $R$  and  $r_{HH}$  at the vinylidene minimum, strongly suggesting that states with these expectation values are vinylidenelike molecular eigenstates.

We also calculated wave functions and expectation values of  $R$  and  $r_{HH}$  using the smaller partial basis of 80 4D functions and the complete basis of 235 4D functions that terminates at the same highest energy state as the smaller 80 4D basis. The results are shown in Fig. 3. As seen the spectrum of vinylidene states in the two sets of calculations is quite similar, and as noted in the previous section the energies of the zero-point vinylidene state and fundamentals are in very good agreement. The major difference between these two sets of results is the much larger density of acetylenic states for the 235 4D basis, as expected. The density of states for this basis, in the energy region shown in Fig. 3, is roughly 1 per  $7\text{ cm}^{-1}$ . (Recall this is the density of states for one of eight symmetry blocks and so the total density of states in this energy region would be roughly 1 per  $\text{cm}^{-1}$ .) This value is roughly twice the corresponding density of states of 1 per  $14\text{ cm}^{-1}$  for the results using the partial basis of 150 4D states. It is interesting to note that interspersed in the spectrum of sharp vinylidene states (as evidenced by expectation values that are very close to equilibrium vinylidene

values) are states with expectation values between those for vinylidene and acetylene. Also, the occurrence of such states appears to be increasing as the energy increases. This indicates that the spectrum of sharp vinylidene states is finite; however, this must be regarded as a tentative observation until converged higher energy calculations can be done. Finally, note that there appear to be more vinylidenelike states in Fig. 2 than in Fig. 3. The reason for this is that the 4D basis used to obtain the results in Fig. 2 contains more vinylidenelike states than do the 4D bases used to obtain the results in Fig. 3.

We have examined a number of wave functions with vinylidenelike expectation values and indeed found they are highly localized in the vicinity of the vinylidene minima. One example, the lowest energy wave function with vinylidene expectation values, is plotted in the upper panels of Figs. 4 and 5. As before,<sup>17</sup> it clearly looks like a ground vibrational state wave function. This wave function is also localized in  $\cos(\theta_1)$  and  $\cos(\theta_2)$  and is symmetric about  $\theta_2$  equal to  $\pi/2$ . By contrast, the analogous plots of the wave function with energy just below that of this vinylidene state, shown in the lower panels of Figs. 4 and 5 displays the character of a highly excited acetylene state. (Note that in these plots the coordinates of all degrees of freedom not plotted have been integrated over. With this procedure the symmetry of wave function in  $\theta_2$  is clearly revealed.)

These results clearly point to the existence of vinylidene eigenstates in qualitative agreement with our previous calculations,<sup>17</sup> which were done with a much smaller basis and different potential energy surface. Indeed, the "spectrum" of expectation values shown in Fig. 2 is quite similar to the one we reported previously; however, the present density of states (using 150 4D basis functions) is considerably larger.

We also did calculations using the 80 4D basis for the  $B'_2$

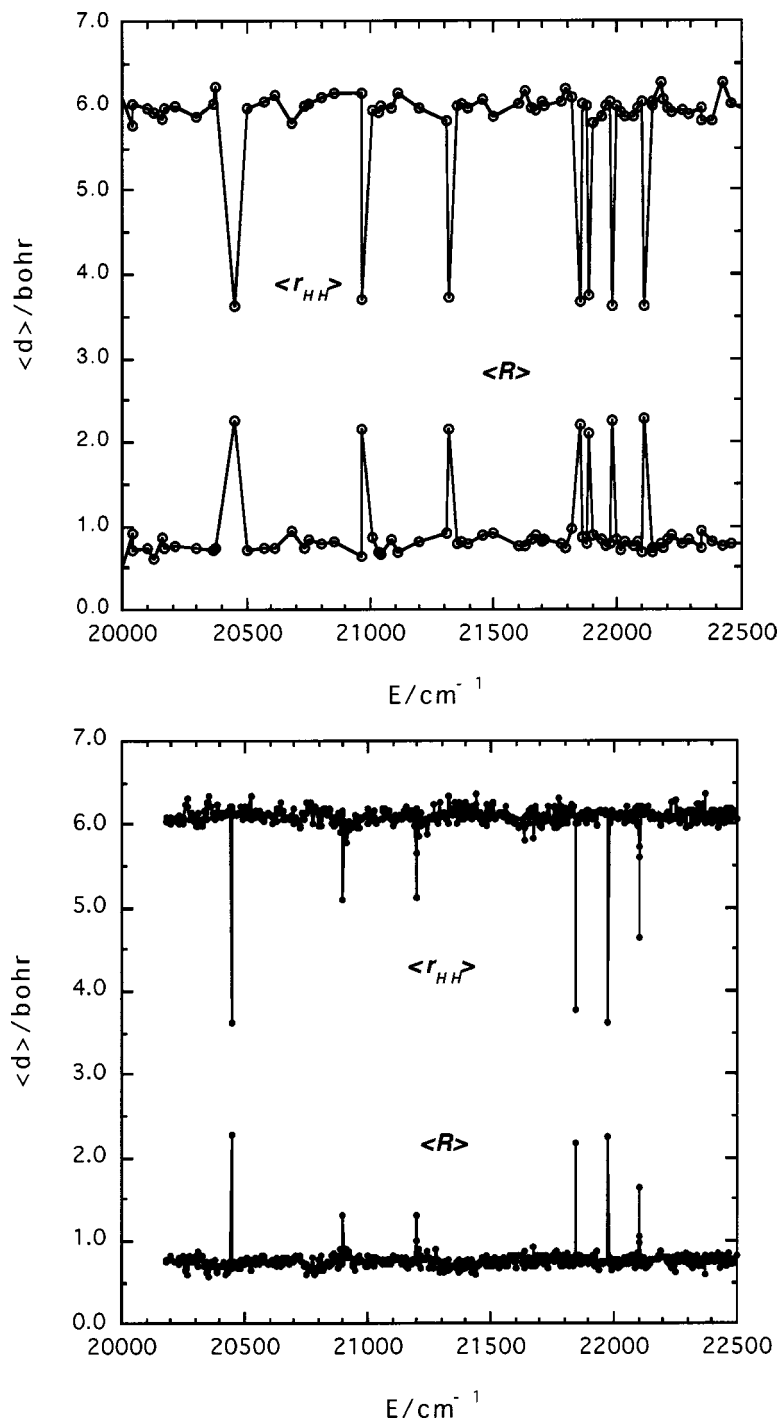


FIG. 3. Expectation values of the radial coordinates  $r_{HH}$  and  $R$  for six degree-of-freedom molecular eigenstates of  $C_2H_2$  (of  $A'_1$  symmetry) in the high-energy region for truncated basis (upper panel) and full basis (lower panel), as explained in the text.

symmetry block of the  $G_8$  point group. These states are anti-symmetric with respect to  $\theta_2$  equal to  $\pi/2$ . We have identified a number of localized vinylidene states that are complementary to the ones shown in Figs. 4 and 5 have been found. For the ground state, the splitting between the anti-symmetric and symmetric pair is roughly  $2 \text{ cm}^{-1}$ . This number has to be taken as a rough estimate of the splitting of course due to the imprecision of our calculations. However, the *existence* of symmetric and anti-symmetric states is rigorous and does point out that the vinylidene spectrum should consist of doublets. This doublet structure would result in an apparent line width of the order of the doublet splitting in a “low resolution” experiment.

Energies and state assignments of some low-lying vinylidene states are given in Table III. Assignments were determined by examining wave functions and also using the normal mode frequencies of vinylidene<sup>10</sup> as a guide. We also give previous results from the experiments of Ervin *et al.*,<sup>1</sup> the planar 5D wave packet/absorbing potential calculations of Schork and Köppel<sup>12</sup> and the second-order perturbation theory calculations of Stanton and Gauss.<sup>6</sup> There is excellent agreement between all results for  $\nu_2$  and  $\nu_3$ . Our calculations for  $\nu_6$  and the  $2\nu_6$  overtone are somewhat below the other calculations and experiment. There is good agreement for the combination band  $\nu_2 + \nu_3$  with the Stanton–Gauss calculations. This state was labeled as a prominent peak in



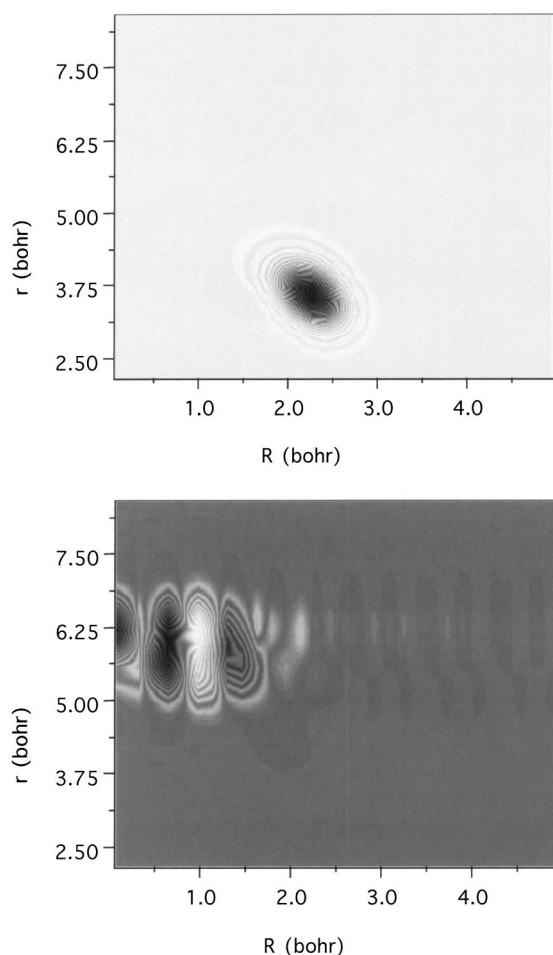


FIG. 4. Image plots of the lowest energy symmetric vinylidene state (upper panel) and the acetylenic state just below it in energy (lower panel) for  $C_2H_2$  in the coordinates  $r=r_{HH}$  and  $R$ .

the photodetachment spectrum but the energy was not reported. We give an estimate of the energy of this state from the spectrum, which is in good agreement with our calculation and with the one of Stanton and Gauss. Our search for the  $\nu_1$  fundamental did not produce a totally conclusive result, so the energy given must be regarded as tentative. (It should be noted that the normal mode frequency of this mode on the potential used in our calculations<sup>10</sup> is  $3131\text{ cm}^{-1}$ , which is in excellent agreement with the one reported by Stanton and Gauss.) In the case of experiment, a weak spectral feature was assigned to  $\nu_1$  based mainly on a calculated normal-mode frequency.

## 2. $C_2D_2$

Large-scale vibrational calculations of eigenvalues and eigenfunctions of the  $A'_1$  symmetry block of  $C_2D_2$  were done using the bases described in detail in the previous section. As with  $C_2H_2$ , expectation values of all coordinates were calculated. Plots of the expectation values  $\langle R \rangle$  and  $\langle r_{DD} \rangle$  are given in Fig. 6. As seen, there are clear signatures of deuterated vinylidene states. The density of states (of the  $A'_1$  symmetry block) in the energy region shown in this figure is roughly 1 state per  $8\text{ cm}^{-1}$ , which is roughly twice the den-

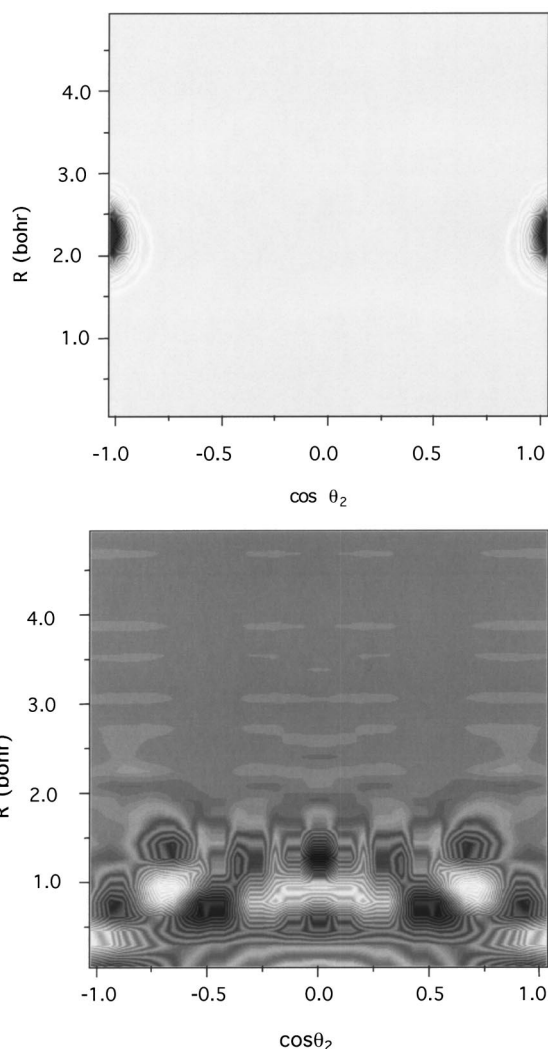


FIG. 5. Image plots of the lowest energy symmetric vinylidene state (upper panel) and the acetylenic state just below it in energy (lower panel) for  $C_2H_2$  in the coordinates  $\cos\theta_2$  and  $R$ .

sity of states of  $C_2H_2$  using a comparable incomplete basis. Based on the increase of the density of states for  $C_2H_2$  using a more complete basis we estimate that the true density of states for  $C_2D_2$  in this energy range for the  $A'_1$  symmetry

TABLE III. Energies for low-lying vinylidene ( $C_2H_2$ ) states from the present 6D calculations along with comparisons with experimental measurements and other calculations. The zero-point energy (ZPE) is given relative to the acetylene minimum. All energies are given in  $\text{cm}^{-1}$ .

States	Sym	Present	5D <sup>a</sup>	2nd P.T. <sup>b</sup>	Experiment <sup>c</sup>
ZPE	$A'_1$	20424	...	...	...
$\nu_6$	$B''_2$	218	301	263	...
$2\nu_6$	$A'_1$	386	473	479	$450 \pm 30$
$4\nu_6$	$A'_1$	633	809	...	...
$\nu_4$	$B''_2$	658	...	...	...
$\nu_4 + \nu_6$	$A'_2$	872	...	...	...
$\nu_3$	$A'_1$	1179	1205	1176	$1165 \pm 10$
$\nu_2$	$A'_1$	1654	1671	1653	$1671 \pm 10$
$\nu_1$	$A'_1$	2783	...	2988	$3025 \pm 30$
$\nu_2 + \nu_3$	$A'_1$	2836	...	2820	$2814 \pm 10^d$

<sup>a</sup>Shork and Köppel, Ref. 12.

<sup>b</sup>Stanton and Gauss, Ref. 6.

<sup>c</sup>Ervin *et al.*, Ref. 14.

<sup>d</sup>Estimate from the spectrum.

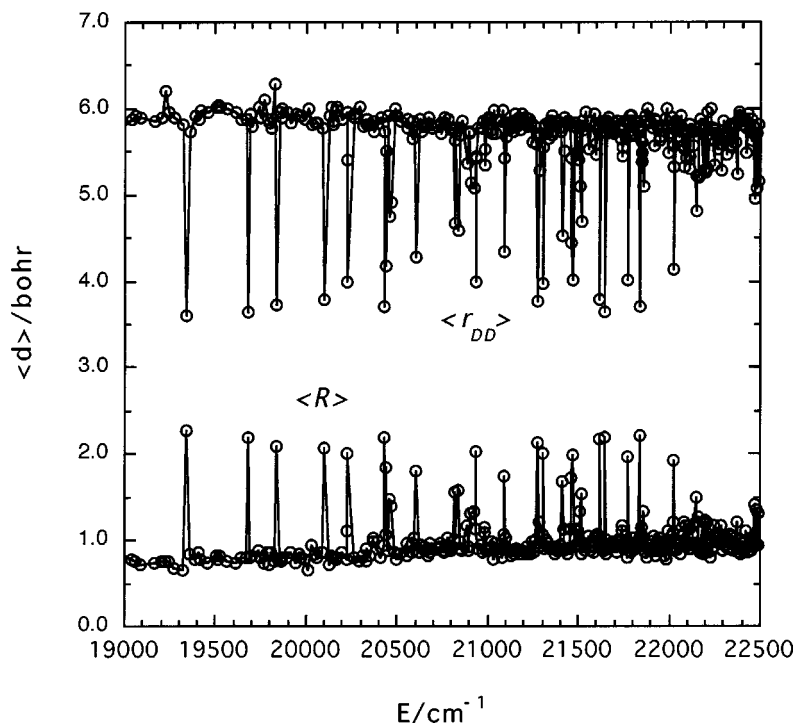


FIG. 6. Expectation values of the radial coordinates  $r_{DD}$  and  $R$  for six degrees-of-freedom molecular eigenstates of  $C_2D_2$  in the high-energy region.

block is roughly 1 per  $4 \text{ cm}^{-1}$  which would imply a complete density of states of  $\sim 2 \text{ per cm}^{-1}$ .

The vibrational energies and assignments for some low-lying states and comparisons with previous results are given in Table IV. The results labeled AIMD are from *ab initio* molecular-dynamics calculations based on an analysis of the power spectrum. There is excellent agreement between all results for the two fundamentals  $\nu_2$  and  $\nu_3$  as well as for the  $2\nu_6$  overtone. The agreement between the theoretical predictions for the  $2\nu_3$  overtone is also excellent; this vibration could not be resolved in the photoelectron experiment and appeared as a shoulder on the  $\nu_2$  fundamental. We are the first to calculate the energy of the  $\nu_1$  fundamental ( $2309 \text{ cm}^{-1}$ ) and the prediction is slightly higher than the experimental estimate. The energy for the  $4\nu_6$  overtone ( $494 \text{ cm}^{-1}$ ) is much less than that calculated by Schork

TABLE IV. Energies ( $\text{cm}^{-1}$ ) for low-lying vinylidene ( $C_2D_2$ ) states of  $A'_1$  symmetry from the present 6D calculations along with comparisons with experimental measurements and other theoretical predictions. The zero-point energy (ZPE) is given relative to the acetylene minimum.

State	Present Work	5D <sup>a</sup>	AIMD <sup>b</sup>	Experiment <sup>c</sup>
ZPE	19341	...	...	...
$2\nu_6$	338	412	327	$370 \pm 30$
$4\nu_6$	494	643	...	...
$\nu_3$	886	889	882	$865 \pm 10$
$\nu_2$	1594	1612	1561	$1590 \pm 20$
$2\nu_3$	1749	1774	1770	...
$\nu_1$	2309	...	...	$2190 \pm 30$
$\nu_2 + \nu_3$	2499	...	...	$2468 \pm 20^d$

<sup>a</sup>Schorck and Köppel, Ref. 12.

<sup>b</sup>Hayes *et al.*, Ref. 6.

<sup>c</sup>Ervin *et al.*, Ref. 1.

<sup>d</sup>Estimate from the spectrum.

and Köppel, but again this band could not be resolved experimentally.

Next we present details and results of the simulation of the photoelectron spectra for  $C_2H_2$  and  $C_2D_2$ . The first step in doing this calculation is to obtain a realistic ground-state vibrational wave function for the anion, which we describe next.

### C. Anion potential and ground-state vibrational wave function

The ground state anion wave function is highly localized and, therefore, should be well described by a conventional, low-order force field. This was obtained using *ab initio* calculations performed using the CCSD(T) method with the aug-cc-pVTZ basis as follows. The equilibrium geometry of the vinylidene anion, and Hessian at this geometry were obtained in Cartesian coordinates using GAUSSIAN 98.<sup>26</sup> We then used this information to generate a grid of energies in terms of the six internuclear distances using methods based on standard finite difference expressions and a step size of 0.001 bohr, as described in detail for a potential for  $H_2O$ .<sup>27</sup> We then fit the resulting data using a full bilinear (28-term) force field in the same coordinates, i.e., six internuclear distances, as used to fit the neutral potential. The absolute average error of the fit was  $0.8 \text{ cm}^{-1}$ . This force field was then used to obtain a full-dimensional ground-state vibrational wave function using the same primitive bases that were used in the calculation of the neutral system.

### D. Photodetachment spectra

Franck–Condon factors were calculated numerically for the ground vibrational state of the anion with the vibrational states of the  $A'_1$  block of the neutral. The resulting spectrum for  $C_2H_2$  is shown in Fig. 7 along with the low resolution

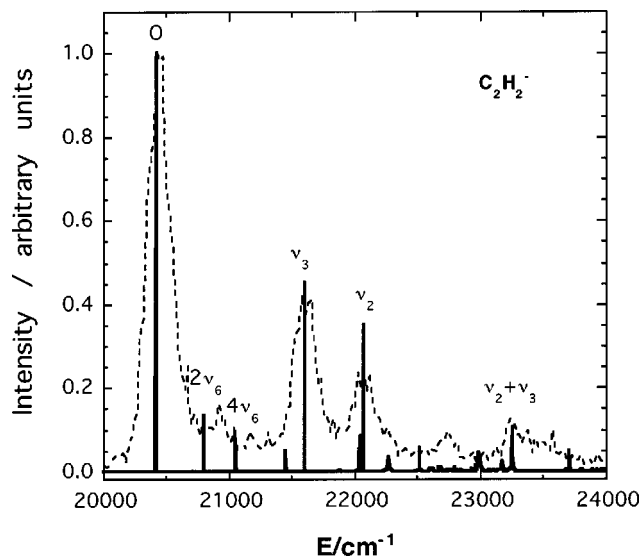


FIG. 7. Franck-Condon factors for the vinylidene anion with molecular eigenstates of acetylene-vinylidene ( $C_2H_2$ ) vs the energy of the neutral and comparison with the experimental photoelectron of Lineberger and co-workers (Ref. 1).

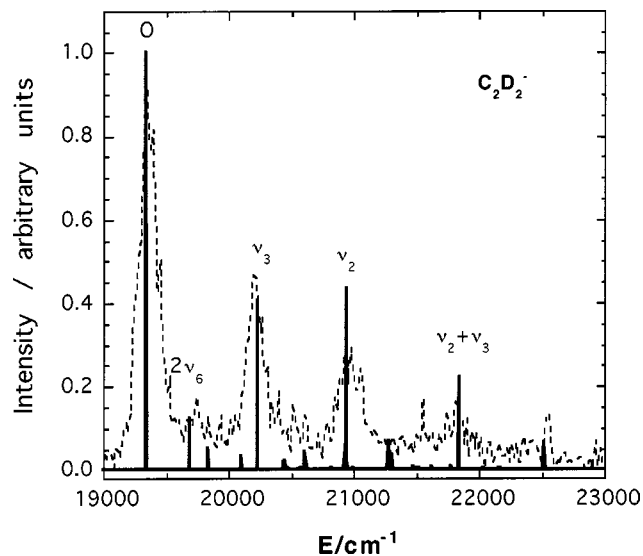


FIG. 8. Franck-Condon factors for the fully deuterated vinylidene anion with molecular eigenstates of acetylene-vinylidene ( $C_2D_2$ ) vs the energy of the neutral and comparison with the experimental photoelectron of Lineberger and co-workers (Ref. 1).

experimental spectrum.<sup>1</sup> (Note only those states in Table III of  $A'_1$  symmetry appear in the photodetachment spectra.) The most intense peak is the overlap of the anion ground state with the ground state of vinylidene neutral. Both the theoretically calculated and the experimentally measured spectra have been normalized with respect to the most intense zero-point energy (ZPE) peak. Also, the zero-point energy of the experimental spectrum has been set such that the largest measurement in this peak coincides with the theoretical ZPE peak. The overlaps of anion ground state with vinylidene states  $2\nu_6$ ,  $4\nu_6$ ,  $\nu_3$ ,  $\nu_2$ , and  $\nu_2 + \nu_3$ , which have the  $A'_1$  symmetry in  $G_8$  CNPI group ( $A_1$  symmetry in  $C_{2v}$  point group), are very prominent and the intensities of those states agree well with the experimental results.

As was done for  $C_2H_2$ , Franck-Condon factors were calculated numerically for the ground symmetric state of the anion with excitation to all states in the  $A'_1$  symmetry block of the neutral for  $C_2D_2$ . The anion potential used was the same as that for the corresponding  $C_2H_2$  calculations. The resulting spectrum along with the experimental one are given in Fig. 8. As labeled in the figure, the most prominent absorptions are (in decreasing order of magnitude) to the ground states and then to states  $\nu_2$ ,  $\nu_3$ ,  $\nu_2 + \nu_3$ , and  $2\nu_6$ . The intensities of these peaks agree well with the experimental measurements.

#### IV. SUMMARY AND CONCLUSIONS

We reported full dimensionality quantum calculations of vibrational eigenstates of  $C_2H_2$  and  $C_2D_2$  to energies above the threshold for formation of vinylidenelike states. A new *ab initio* potential was used in these calculation that is a major improvement over previous ones that describe the isomerization. The eigenstates were obtained using a six degree-of-freedom Hamiltonian in  $C_2-H_2$  diatom-diatom Jacobi coordinates, for zero total angular momentum. They were obtained mainly for the  $A'_1$  symmetry block of the  $G_8$

permutation-inversion point group using a novel truncation-diagonalization procedure that used a series of reduced dimensionality Hamiltonians. These eigenstates are symmetric with respect to a rotation of the CC axis that spans the two equivalent vinylidene minima. Analysis of expectation values and a visual inspection of several wave functions clearly indicates the existence of vinylidenelike molecular eigenstates. In the case of  $C_2H_2$  this analysis was done using three different bases, which indicates the robustness of this conclusion. However, an absolutely definitive verification of this conclusion will require a highly converged calculation of all molecular eigenstates in the high energy regime. Energies of vinylidene and fully deuterated vinylidene states were presented and compared to previous approximate calculations and experiment.

Limited calculations were also done for  $C_2H_2$  for the  $B'_2$  symmetry block; these states are antisymmetric with respect to CC-axis rotation. A small splitting of the order of  $2\text{ cm}^{-1}$  or less was found for these antisymmetric states relative to the symmetric ones which indicates the vinylidene spectrum should consist of closely spaced doublets.

The photodetachment spectra of  $C_2H_2$  and  $C_2D_2$  were also calculated using a realistic, full dimensional ground-state vibrational wave function for the anion, based on an *ab initio* force field. The resulting spectra were directly compared to the experimental spectra, which are not fully resolved and very good qualitative agreement with these spectra was found.

#### ACKNOWLEDGMENTS

The authors thank the Department of Energy (DE-FG02-97ER14782) for financial support. We thank Hua Guo for helpful correspondence and for performing benchmark calculations that were very important in validating our code. We also thank Carl Lineberger for sending the experimental photodetachment spectra.

- <sup>1</sup>K. M. Ervin, J. Ho, and W. C. Lineberger, *J. Chem. Phys.* **91**, 5974 (1989).
- <sup>2</sup>For a review, see M. P. Jacobson and R. W. Field, *J. Phys. Chem. A* **104**, 3073 (2000).
- <sup>3</sup>J. Levin, H. Feldman, A. Baer, D. Ben-Hamu, O. Heber, D. Zajfman, and Z. Vager, *Phys. Rev. Lett.* **81**, 3347 (1998).
- <sup>4</sup>T. Carrington, Jr., L. M. Hubbard, H. F. Schaefer III, and W. H. Miller, *J. Chem. Phys.* **80**, 4347 (1984).
- <sup>5</sup>N.-y. Chang, M.-y. Shen, and C.-h. Yu, *J. Chem. Phys.* **106**, 3237 (1997).
- <sup>6</sup>J. F. Stanton and J. Gauss, *J. Chem. Phys.* **110**, 6079 (1999).
- <sup>7</sup>S. Carter, I. M. Mills, and J. N. Murrell, *Mol. Phys.* **41**, 191 (1980).
- <sup>8</sup>L. Halonen, M. S. Child, and S. Carter, *Mol. Phys.* **47**, 1097 (1982).
- <sup>9</sup>J. F. Stanton (private communication).
- <sup>10</sup>S. Zou and J. M. Bowman, *Chem. Phys. Lett.* **368**, 421 (2003).
- <sup>11</sup>T. Germann and W. H. Miller, *J. Chem. Phys.* **109**, 94 (1998).
- <sup>12</sup>R. Schork and H. Köppel, *J. Chem. Phys.* **115**, 7907 (2001), and references to their earlier work.
- <sup>13</sup>J. A. Bentley, R. E. Wyatt, M. Menou, and C. Leforestier, *J. Chem. Phys.* **97**, 4255 (1992).
- <sup>14</sup>R. L. Hayes, E. Fattal, N. Govind, and E. A. Carter, *J. Am. Chem. Soc.* **123**, 641 (2001).
- <sup>15</sup>T. A. Holme and R. D. Levine, *Chem. Phys.* **131**, 169 (1989).
- <sup>16</sup>S. Zou and J. M. Bowman, *J. Chem. Phys.* **116**, 6667 (2002).
- <sup>17</sup>S. Zou and J. M. Bowman, *J. Chem. Phys.* **117**, 5507 (2002).
- <sup>18</sup>(a) R. Prosimiti and S. C. Farantos, *J. Chem. Phys.* (to be published); (b) *J. Chem. Phys.* **103**, 3299 (1995).
- <sup>19</sup>D. Xu, G. Li, D. Xie, and H. Guo, *Chem. Phys. Lett.* **365**, 480 (2002); D. Xu, R. Chen, and H. Guo, *J. Chem. Phys.* **118**, 7273 (2003).
- <sup>20</sup>L. Liu and J. T. Muckerman, *J. Chem. Phys.* **107**, 3402 (1997).
- <sup>21</sup>J. M. Launay, *J. Phys. B* **10**, 3665 (1977); M. H. Alexander and A. P. DePristo, *J. Chem. Phys.* **66**, 2166 (1977).
- <sup>22</sup>J. Z. H. Zhang, *Theory and Application of Quantum Molecular Dynamics* (World Scientific, Singapore, 1999), pp. 41–45.
- <sup>23</sup>J. M. Bowman and B. Gazdy, *J. Chem. Phys.* **94**, 454 (1991).
- <sup>24</sup>M. J. Bramley and N. C. Handy, *J. Chem. Phys.* **98**, 1378 (1993).
- <sup>25</sup>X.-G. Wang and T. Carrington, Jr., *J. Chem. Phys.* **117**, 6923 (2002), and references therein.
- <sup>26</sup>M. J. Frisch *et al.*, Gaussian, Inc., Pittsburgh, PA, 1998.
- <sup>27</sup>T. Xie and J. M. Bowman, *J. Chem. Phys.* **117**, 10487 (2002).